AIChE

Tapered Element Oscillating Microbalance (TEOM) Studies of Isobutane, *n*-Butane and Propane Sorption in β- and Y-zeolites

Kening Gong and Bala Subramaniam
Center for Environmentally Beneficial Catalysis and Dept. of Chemical and Petroleum Engineering, University of Kansas, Lawrence, KS 66045

Palghat A. Ramachandran
Center for Environmentally Beneficial Catalysis and Dept. of Energy, Environmental and Chemical Engineering, Washington University in St. Louis, St. Louis, MO 63130

Keith W. Hutchenson
DuPont Co., Wilmington, DE 19880

DOI 10.1002/aic.12063
Published online September 28, 2009 in Wiley InterScience (www.interscience.wiley.com).

A TEOM is used to elucidate the adsorption/desorption characteristics of alkylation reactants on USY- and β-zeolites. Equilibrium adsorption isotherms were obtained on USY- and β-zeolites using n-butane, isobutane and propane as proxy reactant molecules ($T = 303–398$ K, adsorbate partial pressure 0–1.2 bar). Analysis of the transient adsorption/desorption profiles of these molecules from either a bed of the zeolite or pelletized particles of the crystals (with mean size < 1 μm) demonstrate that diffusion in the secondary meso-/macroporous structure formed in the packing or the pellets controls the overall sorption rates. The experimental adsorption/desorption profiles from the pelletized zeolites were regressed with available mathematical models to obtain effective meso-/macropore diffusivities for reactant molecules, and nearly perfect fits of the experimental and the modeled profiles. Taking into account the dead volume in the system, a criterion for reliable measurements of either micropore or mesopore diffusivities by the TEOM technique is derived. © 2009 American Institute of Chemical Engineers *AIChE J,* 56: 1285–1296, 2010
Keywords: adsorption, desorption, diffusion, zeolites, TEOM

Introduction

Alkylation of isoparaffins is used commercially to produce nonaromatic gasoline blending material. Conventionally, alkylation units use mineral acids, i.e., sulfuric acid (such as those licensed by DuPont/STRATCO and ExxonMobil) and hydrofluoric acid (such as those licensed by ConocoPhillips and UOP), as catalysts. The main characteristics of these processes are described in detail elsewhere.[1] Because of the safety and environmental issues associated with the sulfuric acid and hydrofluoric acid based alkylation units, there has been a strong driving force for developing novel solid acid catalyzed alkylation processes.

The grand challenge in this regard is the development of stable and durable solid acid catalysts. Y- and β-zeolites are known to possess excellent initial activity and C_8 alkylates

Correspondence concerning this article should be addressed to B. Subramaniam at bsubramaniam@ku.edu

selectivity.[2–6] However, they deactivate rapidly due to catalyst fouling. Understanding the fundamentals of the adsorption, desorption and mass transfer rates of hydrocarbons in these catalysts is key to screen potential solid acid catalysts and rationally determine operating conditions.[2,3,7,8] This work uses a tapered element oscillating microbalance (TEOM) to elucidate the adsorption/desorption characteristics of some light hydrocarbons on these zeolites.

In addition, this work investigates the ability of TEOM as a tool to measure micropore and macropore diffusivities for commercially available large-pore (12-ring) zeolites with small crystal sizes (<1 μm) and focuses on the deeper understanding of the limitations of this instrument for diffusivity measurement. Measuring the diffusivities of light hydrocarbons in large-pore zeolites with small crystals is rather challenging using classic macroscopic methods such as gravimetric uptake and zero length column (ZLC) techniques due to the high diffusivity and short diffusion length in small crystals.[9] More reliable studies with large crystals (usually > 40 μm) have revealed that in almost all studies using small micron-sized crystals, the dynamics are likely controlled by extracrystalline rather than intracrystalline diffusion.[9]

The TEOM technique was originally designed for *in situ* monitoring of particulate concentrations in the effluents of combustion systems.[10,11] In the early 1990's, the Rupprecht and Patashnick TEOM 1500 PMA was developed for laboratory studies of gas-solid reactions. Since then, the advantages of the TEOM technique have been demonstrated in the investigations of coking kinetics,[12–14] influence of coke deposition on selectivity,[15] combined diffusion, adsorption, reaction and coking.[14,16,17]

Additionally, a few published articles have addressed the topic of adsorption/desorption equilibria and kinetics using the TEOM technique, mainly aimed at measuring the intracrystalline diffusivities of hydrocarbons in zeolitic materials.[18–24] Most of these measurements were conducted with small commercially available crystals (usually < 1 μm) or with the pelletized samples made of such small crystals. With such materials, detailed investigations of dynamics under a wide variety of conditions (e.g., by varying sample size and flow rate) must be carried out, if possible, in order to correctly identify the rate-limiting step for mass transfer. However, such investigations were typically ignored or vastly simplified. For example, Chen et al.[18] and Rebo et al.[19] chose certain sample sizes ($\sim$7–8 mg) in the measurements of uptake dynamics of hydrocarbons in HZSM-5 catalyst to obtain tolerable signal/noise ratio and to lower the concentration gradients/pressure drop; however, the effects of varying the sample size and the carrier gas flow rate were not thoroughly investigated. When measuring adsorption/desorption rates of hydrocarbons in a commercial fluid catalytic cracking (FCC) catalyst and a pure rare-earth exchanged zeolite Y catalyst, Lee et al.[22] studied the effect of carrier gas flow rate on the adsorption/desorption dynamics, but did not conduct experiments with various sample sizes.

This work is aimed at a better understanding of the rate-controlling steps underlying adsorption/desorption dynamics, and special attention was paid to the usually neglected factors of meso-/macropore and bed diffusion. Such a fundamental understanding is essential to rationally design catalysts with maximum effectiveness.

Experimental

Principles

A schematic diagram of a TEOM is shown in Figure 1. At the center of the TEOM is a tapered element (TE), which is used to restrain the solid sample in the bed with inert quartz wool, as well as to measure the mass change of the sample. The carrier gas enters the top part of the tapered element, proceeds downward through the hollow section and then passes through the packed bed, where it comes into intimate contact with the solid samples. A purge gas passes down around the tapered element to guide and direct the carrier gas stream as it exits from the tapered element (such a design helps to prevent effluent gas diffusing back into the tapered element). Inside the TEOM, there are two heating zones for the specific need of temperature control. One (preheating zone) controls the gas-stream temperature upstream of the tapered element while the other (main heating zone) controls the temperature in the tapered element and the packed bed.

The top of the tapered element is fixed, so that the whole element can oscillate in a clamped-free mode. A detailed introduction of the oscillating mechanism of the TEOM technique can be found elsewhere.[25] The natural oscillating frequency of the tapered element increases when the mass of the solid in the packed bed decreases, and *vice versa*. The system obtains accurate and time resolved values of mass change, by simply comparing the measured natural oscillating frequency to the one recorded at the beginning of the experiment. The system measures the mass change between two time points "0" and "1" using the following equation

$$\Delta m = K\left[\frac{1}{f_1^2} - \frac{1}{f_0^2}\right] \tag{1}$$

where Δm is the mass change, K is the spring constant of the tapered element, f_0 is the natural oscillating frequency at time "0", and f_1 is the natural oscillating frequency at time "1". This instrument provides excellent sensitivity, allowing mass changes as little as 1 μg to be detected.

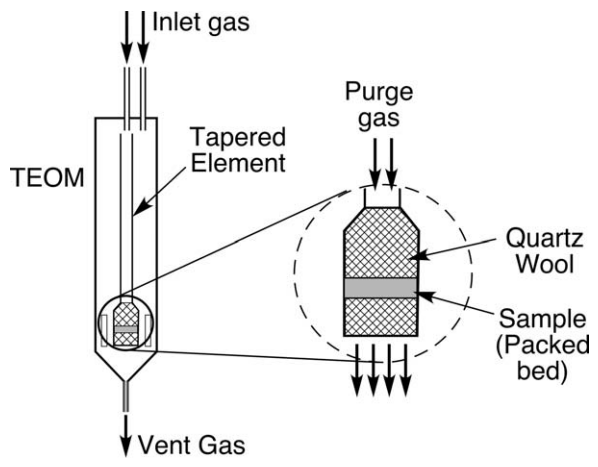

Figure 1. Schematic diagram of a TEOM.

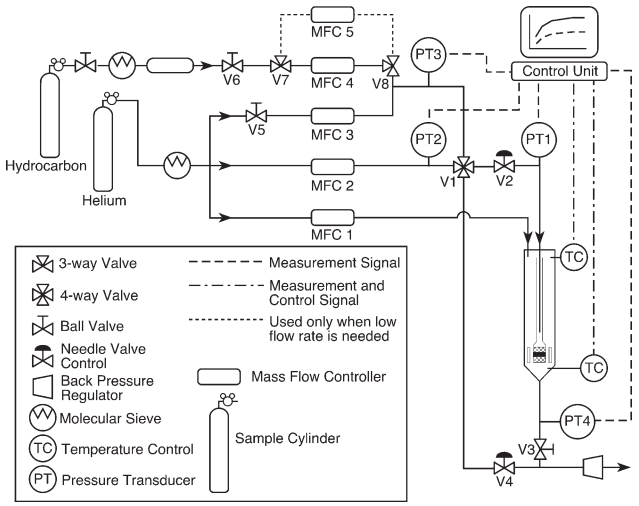

Figure 2. Schematic diagram of the experimental setup.

Procedure

A schematic diagram of the experimental setup is shown in Figure 2. The following procedure is employed to obtain the adsorption capacity and the rates of adsorption/desorption.

Prior to the experiments, zeolite crystals or mesoporous materials are packed firmly by quartz wool in the tapered element, and the samples are heated at 10 K/min in flowing zero grade air at 100 sccm to the desired pretreating temperature of 773 K, which is maintained for 5 h. Then the sample is cooled to the temperature of interest in a helium flow of 400 sccm. Another stream carrying hydrocarbon gas is directly connected to a vent outlet without flowing through the tapered element.

After a stable mass baseline is obtained, the 4-way injection valve (valve 1) is switched to make the stream containing hydrocarbon gas flow through the tapered element, while the pure helium stream is connected to the vent. The problem of pressure imbalance when switching the 4-way valve has been discussed in detail elsewhere.[22,24] The needle valves 2 and 4 are used to equalize the flow resistances downstream of the switching valve 1 such that the flow rate and the pressure drop in each carrier gas steam are virtually undisturbed when valve 1 is switched. The pressure transducers at the entrance and the exit of the tapered element are used to continuously monitor the pressure change. Once the adsorption equilibrium has been attained after a certain period of time (usually 100 s), valve 1 is switched back to its initial position and desorption commences. By this procedure, the total mass change is measured following a step change (either increase or decrease) in hydrocarbon concentration for a certain loading of catalysts.

In addition, the extent of mass change caused by the gas density variation in the void space within the tapered element and due to surface adsorption is determined in a blank run performed with nonporous quartz particles (identical in size and amount as the substrates of interest) at identical operating conditions. Such blank runs have been demonstrated to be crucial to obtain the intrinsic mass change profiles using TEOM in other studies.[14,17,26] The intrinsic mass change due to adsorption is determined by subtracting the mass change due to gas density variation and surface adsorption from total mass change, as shown in Figure 3a. Similar experiments were performed under different adsorbate partial pressures at the same temperature with quartz particles and zeolites. The intrinsic equilibrium adsorption isotherm was obtained through subtraction, as shown in Figure 3b.

The partial pressure of hydrocarbon is controlled by setting the gas flow rates. Helium is used as both the purge and carrier gas. The gas flow rates are controlled by an OMEGA FMA-700 series mass flow controllers. The carrier gas flow rates are each set at 400 sccm (unless otherwise mentioned), and the purge gas flow rate is maintained at 50 sccm. The pressures at the inlet and outlet of the tapered element are carefully monitored to avoid significant pressure drop ($\Delta P \leq 0.1$ bar) along the sample bed. The temperature set point in the isothermal TEOM sample bed ranges from 303–473 K. The pressures, temperatures, gas flow rates and mass changes of the sample are recorded continuously during the experiment. The time interval to measure the natural oscillating frequency is approximately 0.8 s, and such a high time

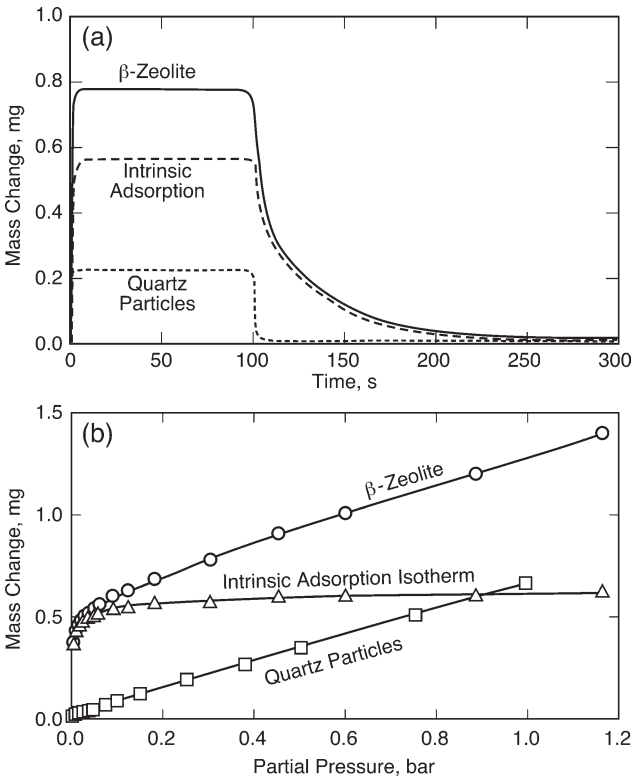

Figure 3. Procedures for the measurement of intrinsic adsorption/desorption profiles and intrinsic equilibrium adsorption isotherms: (a) Intrinsic adsorption/desorption profiles of isobutane on β-zeolite (T = 323 K; P_{iC4} = 0.304 bar; P = 1.4 bar; β-zeolite loading = 6.4 mg); (b) Intrinsic isobutane adsorption isotherm on β-zeolite (T = 323 K; P = 1-1.5 bar; β-zeolite loading = 6.4 mg).

Table 1. Properties of β-zeolite and USY-zeolite

Properties	β-zeolite	USY-zeolite
Si/Al ratio[a] (mol/mol)	13.3	2.9
Average crystal size[a] (μm)	<1	<1
Agglomerate size, intergrown[a] (μm)	4–30	4–30
Total surface area[b] (m^2/g)	605.9	665.2
Surface area with pores < 2 nm[b] (m^2/g)	542.0	610.3
Surface area with pores > 2 nm[b] (m^2/g)	63.9	54.9
Total pore volume[b] (cc/g)	0.286	0.312
Pore volume with pores < 2 nm[b] (cc/g)	0.222	0.251
Pore volume with pores > 2 nm[b] (cc/g)	0.064	0.061
Acidity[c] (μmole NH_3/g catalyst)	291.2	466.0

[a]Provided by manufacturer (GRACE Davison)
[b]Provided by DuPont using BET
[c]Provided by ConocoPhillips using TPD

resolution makes the TEOM capable of measuring relatively fast adsorption/desorption kinetics.

Characterization of adsorbents and adsorbates

The β-zeolite (SMR 5-9858-01062, Si/Al ratio = 13.3) and USY-zeolite (SMR 5-9858-01061, Si/Al ratio = 2.9) were supplied by GRACE Davison. Table 1 summarizes the key properties of the samples. SEM images show that both types of materials have very small crystal size (average crystal diameter < 1 μm). The crystals tend to form small particles (diameter 4–30 μm) through self-aggregation. N_2 BET area and pore volume characterizations of zeolites were performed at DuPont by a Micromeritics ASAP 2405N automatic sorption analyzer. The surface areas in micro/zeolitic pores (pore diameter < 2 nm) account for 89.5% and 91.7% of the total surface areas for β-zeolite and USY-zeolite, respectively. The pore volumes in mesopores/macropores (pore diameter > 2 nm) account for 22.3% and 19.6% of the total pore volumes for β-zeolite and USY-zeolite, respectively. In the meso-/macroporous range, it is found that 42.7% and 54.6% of the pore volume reside in 2–5 nm pores for the β-zeolite and USY-zeolite, respectively, implying that the meso- and macropores have relatively small average diameter through aggregation. Accordingly, the zeolites in this study are treated as particles with a bimodal pore size distribution. In addition to the intracrystalline diffusion resistance, the extracrystalline mass transfer resistances in the self-aggregated particles and in the packed bed (similar to the self-aggregation) are considered.

To determine the acidity values of β-zeolite and USY-zeolite, ammonia TPD (temperature-programmed desorption) experiments were conducted at ConocoPhillips using a Micromeritics ASAP 2910 sorption analyzer equipped with a thermal conductivity detector (TCD), and the results are listed in Table 1.

A DuPont-Q500 thermal gravimetric analyzer (TGA) was used to measure the nonstructural water content in β-zeolite. The sample was heated at 10 K/min to 473 K in a flow of argon. It is found that the water content in β-zeolite is 10–13 wt %. Similar observations were reported by Platon et al.[4] who noted that the water content in two β-zeolite samples is in the range of 8–10 wt % when the samples were heated at 10 K/min to 523 K in an argon-purged environment. Such results indicate that zeolite samples contain a significant amount of nonstructural water. Therefore, in the adsorption/desorption experiments, the adsorbent is weighed after being dried at 383 K for 5 h in an argon-purged oven. All the reported adsorbent weights in this study are on a dry weight basis.

Ultra high purity helium (purity > 99.999%, Airgas) is used as carrier gas and purge gas. The adsorbates employed are research grade gases (isobutane purity > 99.995%, *n*-butane purity > 99.98%, and propane purity > 99.993%) from Matheson Tri-gas.

Mathematical Modeling of Equilibrium Adsorption Isotherms and Sorption Kinetics

Mathematical modeling of equilibrium adsorption isotherms

For microporous materials such as zeolites, the Langmuir model usually provides a reasonably good description of the measured equilibrium adsorption isotherms. This model is developed based on the following assumptions: (a) there is no surface heterogeneity; (b) only localized adsorption occurs, and there is no interaction between the adsorbed molecules; and (c) each site can be occupied by only one molecule. The Langmuir model is defined as

$$q = \frac{q_s b p}{1 + bp} \tag{2}$$

where q is the concentration in the adsorbed phase, q_s is the saturation concentration in the adsorbed phase, b is Langmuir equilibrium constant, and p is the partial pressure of adsorbate.

When there exist two different (homogeneous) types of adsorption sites in the microporous materials, the dual-site Langmuir model usually leads to a better description.[26,27] The dual-site Langmuir model is defined as

$$q = \frac{q_{s1} b_1 p}{1 + b_1 p} + \frac{q_{s2} b_2 p}{1 + b_2 p} \tag{3}$$

where q_{s1} and q_{s2} are the saturation concentrations in each type of adsorption site, b_1 and b_2 are Langmuir equilibrium constants for each sorption site.

A numerical routine (''fminsearch'' function in Matlab) was used to search for the equilibrium isotherm parameters that minimize the value of the following objective function

$$S_{TG} = \sum_{i=1}^{n} \left(m_i^{\exp} - m_i^{cal} \right)^2 \tag{4}$$

where $m^{\exp}$ is the adsorbed amount that is measured in the experiments, m^{cal} is the adsorbed amount that is calculated with a given set of parameters. Subscript i denotes the discrete value corresponding to each partial pressure, and n is the total number of discrete data points (i.e., partial pressures) employed in the evaluation.

Mathematical modeling of sorption kinetics

As mentioned earlier, the zeolite crystals form small particles through self-aggregation. The particle diameter (4–30 μm) is measured with a SEM by spreading the sample particles on a smooth metal surface. When packed in the TEOM, larger particles can be formed through compaction

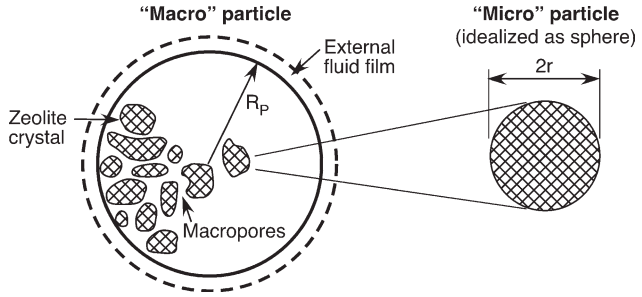

Figure 4. Schematic diagram of a zeolite particle.

and aggregation. To investigate the effects of such aggregation on adsorption/desorption dynamics and diffusivity measurements, controlled-size cylindrical pellets of the zeolite samples were formed with a high-pressure press and systematically studied in the TEOM. As shown in Figure 4, the aforementioned particles and pellets exhibit a bimodal pore-size distribution, with the smaller mean pore size representing the micropores (< 2 nm) of the zeolite crystals and the larger mean pore representing the mesopores (2–50 nm) or macropores (>50 nm) formed by the aggregation of the crystals.

In this work, the bed-length effect was found to be negligible when sufficiently small sample sizes and sufficiently high carrier gas flow rates are used in the experiments (as discussed in the section "Effects of Bed-length and Film Mass Transfer Resistance"). Only in such a case is it justifiable to employ a single particle model to adequately describe the observed adsorption/desorption dynamics. In the single particle model, the external fluid film resistance may also be assumed to be negligible at relatively high carrier gas flow rates.

Diffusion resistance in either the bed or a single particle can occur in either the intracrystalline phase (consisting of the micropores) or the extracrystalline phase (consisting of the meso- and macropores). The rate-limiting step for adsorption/desorption dynamics is determined by the relative magnitudes of the diffusional time constants [effective diffusivity/(diffusion path length)^2] in these channels. If the ratio of diffusional time constants $[(D_{\text{micro}}/r_c^2)/(D_{\text{meso/macro}}/R_p^2)] \gg 1$, the rate-limiting step is mesopore/macropore diffusion. If the ratio is $\ll 1$, then micropore diffusion controls the overall rate of adsorption/desorption. The rate-limiting step must be properly identified for reliable interpretation of the sorption dynamics and the estimation of intrinsic diffusivities. Hence, models for micropore diffusion control and for meso/macropore diffusion control are presented, respectively in the following paragraphs and these models are used later in the text to identify the rate-limiting step.

Micropore Diffusion Control. In this scenario, the diffusion rate through the extracrystalline space in the aggregated particles, as well as the mass transfer rate at the crystal surface are rapid, and the overall rate of adsorption/desorption is controlled by intracrystalline diffusion.

When the adsorption/desorption profiles are measured over large step changes of adsorbate concentration, the nonlinearity of the equilibrium adsorption isotherm should be considered, and the assumption of constant diffusivity is usually not valid. Assuming that the equilibrium adsorption isotherm is described well by a Langmuir-type equation, the intracrystalline diffusivity can be written in the form[9]

$$D_c = \frac{D_0}{1 - q/q_s} \tag{5}$$

where D_c is the intracrystalline diffusivity, and D_0 is the corrected intracrystalline diffusivity. Accordingly, the transient mass balance in a spherical microparticle is as follows

$$\frac{\partial q}{\partial t} = \frac{D_0}{r^2}\frac{\partial}{\partial r}\left(\frac{r^2}{1 - q/q_s}\frac{\partial q}{\partial r}\right) \tag{6}$$

where r is the radial distance in the zeolite crystal. The relevant initial condition is

$$t < 0, \quad c = c_0, \quad q = q_0 \tag{7a}$$

where c is the concentration in external fluid phase, c_0 is the initial value of c, and q_0 is the initial value of q. Note that c and q are related by a Langmuir equation. The boundary conditions are

$$t \geq 0, \quad c = c_\infty, \quad q(r_c, t) \to q_\infty \tag{7b}$$

$$\left.\frac{\partial q}{\partial t}\right|_{r=0} = 0, \quad \forall\, t \tag{7c}$$

where c_∞ is the value of c as $t \to \infty$, q_∞ is the value of q as $t \to \infty$, and r_c is the radius of zeolite crystal.

The diffusivity is obtained by fitting the transient experimental data to the numerical solution of Eqs. 6 and 7.

Mesopore/Macropore Diffusion Control. In this scenario, the intracrystalline diffusion is relatively rapid, and the adsorption/desorption rate is controlled by diffusion through the mesopores/macropores of the aggregated particles.

A mathematical model was developed to describe the diffusion in the cylindrical pellets over a small concentration step. The key assumptions include, (a) the intracrystalline diffusion is rapid, (b) the external transport resistances are negligible, (c) the pellets are isothermal, and (d) the equilibrium adsorption isotherm is linear with concentration under differential concentration steps. The transient intrapellet mass balance equation is

$$\frac{\partial c}{\partial t} = D_e\left(\frac{1}{R}\frac{\partial}{\partial R}\left(R\frac{\partial c}{\partial R}\right) + \frac{\partial}{\partial Z}\left(\frac{\partial c}{\partial Z}\right)\right) \tag{8}$$

The initial condition is

$$c(Z, R, 0) = c_0 \tag{9a}$$

and the boundary conditions are

$$c(Z, R_p, t) = c_\infty \tag{9b}$$

$$c(Z_{\pm 0.5L}, R, t) = c_\infty \tag{9c}$$

$$\frac{\partial c(Z, 0, t)}{\partial R} = 0 \tag{9d}$$

where D_e is the effective mesopore/macropore diffusivity, R is the radial coordinate in the pellet, Z is the distance coordinate,

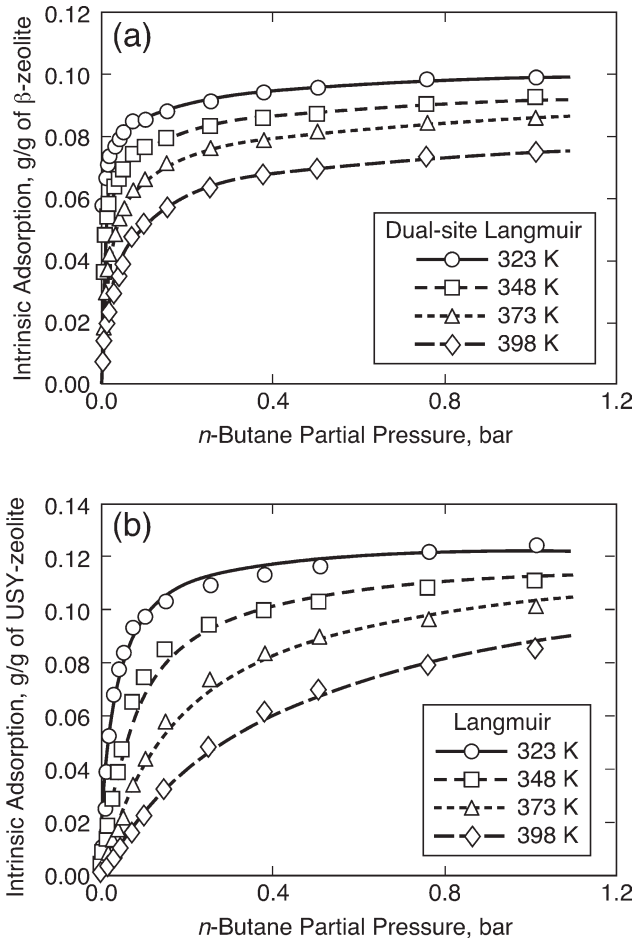

Figure 5. Intrinsic adsorption equilibrium isotherms of *n*-butane in zeolites (a) in *β*-zeolite, and (b) in USY-zeolite.

R_p is the pellet radius, and L is the cylinder length. The effective mesopore/macropore diffusivity may be written as[9]

$$D_e = \frac{\varepsilon_p D_p}{\varepsilon_p + (1-\varepsilon_p)(dq^*/dc)} \tag{10}$$

where D_p is the pore diffusivity, ε_p is the porosity of the pellet, q^* is the equilibrium adsorbed phase concentration, and dq^*/dc is the slope of the equilibrium adsorption isotherm.

The partial differential equations along with the initial and boundary conditions were solved in Femlab that employs a finite element method. The experimental adsorption/desorption profiles were regressed with the model solution to obtain the effective mesopore/macropore diffusivities.

Results and Discussion

Intrinsic equilibrium adsorption isotherms

Experiments of *n*-butane, isobutane, and propane adsorption/desorption on *β*-zeolite and USY-zeolite were performed under adsorbate partial pressures of 0–1.2 bar at temperatures of 303–398 K, and the corresponding equilibrium adsorption isotherms (the amounts adsorbed are normalized to the weight of adsorbent) are shown in Figures 5, 6, and 7. In this study, *n*-butane and propane were used as proxies for 1-butene and propene, respectively, to avoid oligomerization of olefins in the zeolites.[4,14]

Under the operating conditions studied, the equilibrium adsorption isotherms of *n*-butane, isobutane, and propane in both *β*-zeolite and USY-zeolite exhibit type I shape in the Brunauer classification. At sufficiently low-partial pressures, the isotherms are in the linear region (Henry's law region), which is also confirmed by nearly identical adsorption and desorption rates in the corresponding adsorption/desorption profiles. At sufficiently high partial pressures, the equilibrium adsorption isotherms approach saturation. This type of equilibrium isotherm is typical for adsorption in microporous materials (e.g., zeolites and charcoals), and a monolayer coverage is postulated at equilibrium.[28]

There are a few empirical models that are commonly used to fit type I equilibrium adsorption isotherms, including Langmuir, Toth, and Unilan models. Among these, the simplest and most widely used one is the Langmuir model. In this study, it is found that either the Langmuir or the dual-site Langmuir model leads to good descriptions for the equilibrium adsorption isotherms of C_3-C_4 alkanes in *β*- and USY-zeolites. In addition, both the Langmuir and dual-site

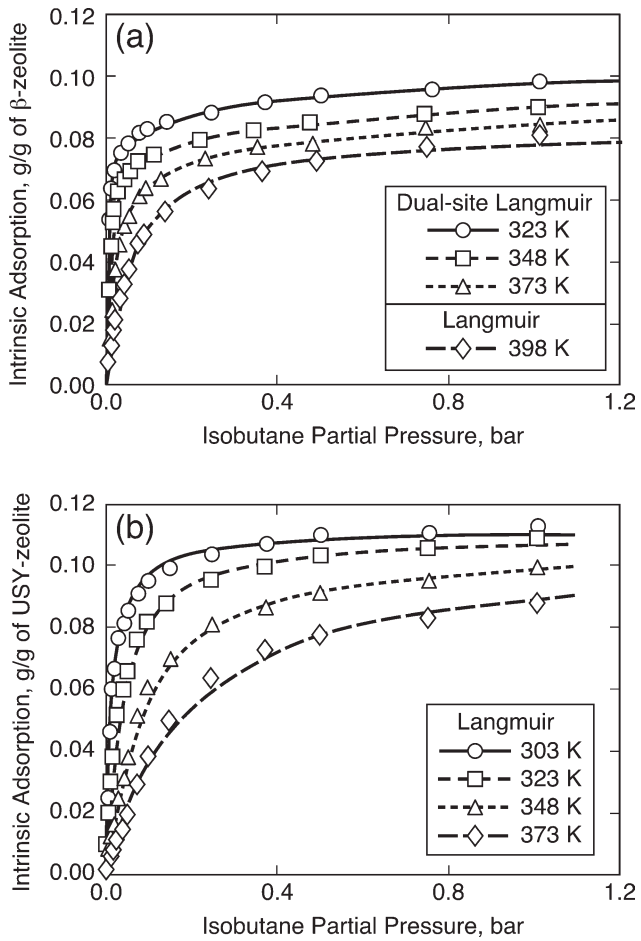

Figure 6. Intrinsic equilibrium adsorption isotherms of isobutane in zeolites (a) in *β*-zeolite, and (b) in USY-zeolite.

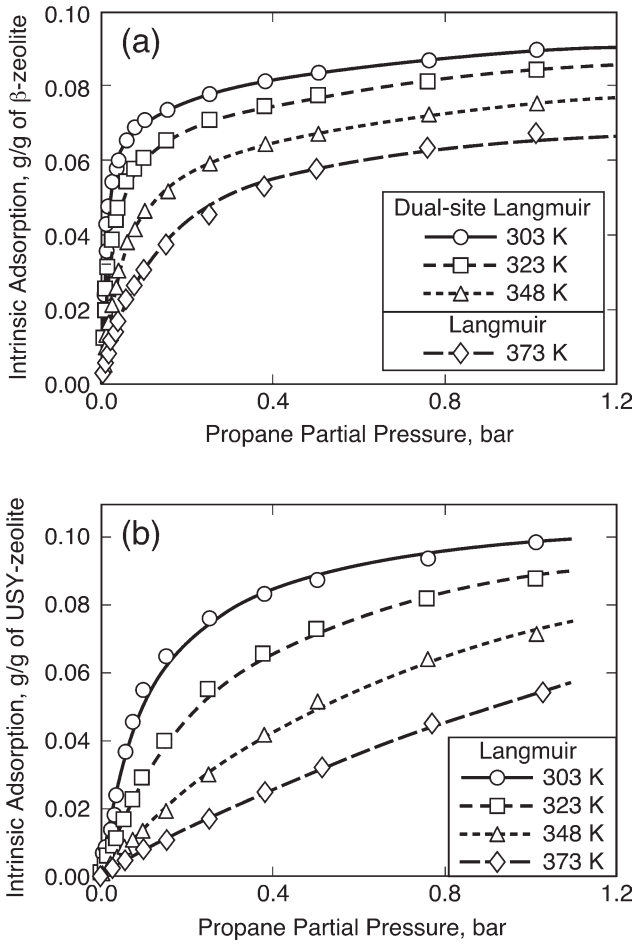

Figure 7. Intrinsic equilibrium adsorption isotherms of propane in zeolites (a) in β-zeolite, and (b) in USY-zeolite.

Langmuir models provide somewhat simplified and straightforward physical interpretations for the adsorption phenomena observed.

It is found that the equilibrium adsorption isotherms of *n*-butane, isobutane, and propane in USY-zeolite are fitted well by the Langmuir model. However, the Langmuir model does not provide good descriptions for the equilibrium isotherms of these light alkanes in β-zeolite at relatively low temperatures. Instead, a good agreement with the experimental results is achieved by using the dual-site Langmuir model, suggesting the existence of two types of adsorption sites in β-zeolite. Dual-site Langmuir models have been widely used to account for the adsorption on two distinctly different adsorption sites. For example, Zhu and his coworkers[26] found that the dual-site Langmuir model provides an excellent description of the equilibrium adsorption isotherms of propane, isobutane, and *n*-butane in silicalite-1 at low temperatures (<373 K); Barcia et al.[27] demonstrated that the dual-site Langmuir model is suitable for the correlation of equilibrium adsorption isotherms of hexane isomers in β-zeolite pellets.

The fitted results of the equilibrium adsorption isotherms of *n*-butane, isobutane, and propane in β-zeolite and USY-zeolite are shown in Table 2. It is found that the saturation capacities of these systems are in the range of 0.07–0.14 g/g of adsorbent. Such values are in good agreement with the published data on similar systems. For example, the measured saturation capacities of isobutane in large-pore 13X zeolite by the static volumetric method are in the range of 0.08–0.11 g/g of adsorbent at 298–373 K;[29] and the measured saturation capacities of propane in 13X zeolite are in the range of 0.09–0.10 g/g of adsorbent at 279–308 K.[30] The saturation capacity of USY-zeolite is 5–30% greater than that of β-zeolite, and this finding is in reasonably good agreement with the BET characterization results (i.e., the total surface area of USY-zeolite is approximately 10% higher than that of β-zeolite). Under the same conditions, the Langmuir constant on β-zeolite is greater than that on USY-zeolite, implying that pore size possibly has a significant effect on the adsorption affinity in the microporous materials. In this study, the zeolite pore sizes are comparable to the adsorbate molecule sizes (the kinetic diameters of *n*-butane, isobutane, and propane are in the range of 0.4–0.5 nm, while the pore diameters of β-zeolite and USY-zeolite are in the range of 0.5–1.2 nm). Under such conditions, adsorption occurs by attractive force from the pore wall.[31]

In the investigation of equilibrium adsorption isotherms of light alkanes (including *n*-butane, isobutane, and propane) in silicalite-1, Zhu et al.[26] found that the saturation capacities of silicalite-1 decrease when temperature increases. However, such a trend was not observed in our study. Instead, the results of our work are in good agreement with the findings by Lee and coworkers.[22] They found that the saturation adsorption capacities of hydrocarbons in Y-zeolite are essentially independent of temperature in the 373–473 K range.

The adsorption affinity of the butane isomers is much stronger than that of propane under the same conditions, indicating that the molecular size has a significant impact on the adsorption affinity. In addition, the influence of branching is studied by comparing the fitted parameters of equilibrium isotherms between the butane isomers. The adsorption affinity of *n*-butane is greater than that of isobutane. A similar trend was observed by other researchers. For example, Barcia et al.[27] found that *n*-hexane has the strongest adsorption strength in β-zeolite among hexane isomers, followed by monobranched and dibranched isomers. Such results show that a larger kinetic diameter (the kinetic diameter of isobutane is larger than that of *n*-butane) does not necessarily correspond to a higher adsorption affinity under the same conditions.

Heat of adsorption is calculated by correlating the Langmuir constants with the Arrhenius equation. In this study, the heat of adsorption possesses noticeable uncertainty (as large as $\pm$4 kJ/mol), and similar uncertainties were observed by Lee and coworkers.[22] These results indicate that the TEOM is probably not suitable for identifying the subtle differences in the adsorption heat among alkane isomers or alkanes with very close carbon numbers when a very small amount of sample is used in the experiments to minimize the impact of the concentration gradient in the packed bed (see the section "*Effects of Bed-length and Film Mass Transfer Resistance*"). To eliminate this limitation, larger amounts of sample should be used to minimize the impact of gas density change and thereby the systematic errors.

Table 2. Summary of the Parameters Obtained from the Analysis of Equilibrium Adsorption Isotherms

Adsorbate	Catalyst	T (K)	q_{max1} (g/g)	b_1 (1/bar)	q_{max2} (g/g)	b_2 (1/bar)	$-\Delta H_{ads1}$ (kJ/mol)	$-\Delta H_{ads2}$ (kJ/mol)
propane	USY-zeolite	303	0.111	8.3			37 ± 4	
		323	0.115	3.3				
		348	0.136	1.1				
isobutane	USY-zeolite	303	0.111	70.9			35 ± 4	
		323	0.111	27.0				
		348	0.108	10.9				
		373	0.106	5.2				
n-butane	USY-zeolite	303	0.127	102.3			39 ± 4	
		323	0.126	34.3				
		348	0.122	12.4				
		373	0.124	5.1				
		398	0.127	2.3				
propane	β-zeolite	303	0.071	128.2	0.029	1.8	38 ± 4	19 ± 4
		323	0.069	51.5	0.035	0.8		
		348	0.064	21.3	0.035	0.7		
		373	0.074	7.0				
isobutane	β-zeolite	323	0.077	444.9	0.025	3.6	47 ± 4	33 ± 4
		348	0.075	143.4	0.027	1.1		
		373	0.075	48.5	0.026	0.7		
		398	0.082	16.2				
n-butane	β-zeolite	323	0.079	498.5	0.024	5.0	44 ± 4	39 ± 4
		348	0.072	182.3	0.024	4.4		
		373	0.070	66.8	0.023	2.7		
		398	0.072	23.6	0.023	0.3		

However, in this study, the main goal is to investigate the adsorption/desorption rates of hydrocarbons in zeolites and this requires the use of rather small sample sizes.

Intrinsic adsorption/desorption dynamics

Effects of Bed-length and Film Mass Transfer Resistance. In order to properly identify the dominant mass transfer resistance in the TEOM experiments, systematic investigations of the adsorption/desorption dynamics were undertaken under carefully controlled conditions. The bed-length effect on the overall adsorption/desorption dynamics was tested by varying both the packing length and, at each bed length, the carrier gas flow rate as well. In the study of hydrocarbon adsorption/desorption in a commercial FCC catalyst and a pure rare-earth exchanged zeolite Y sample using a TEOM, Lee et al.[22] varied the carrier gas flow rate at a fixed bed length and concluded that the concentration gradient down the fixed bed is negligible beyond the carrier gas flow rate at which the dynamic profiles became invariant. Based on this assumption, the environment surrounding each catalyst particle in the fixed bed was considered to be identical. Clearly, this assumption is valid only below a certain bed length (''differential'' operation).

Indeed, further experimental investigation into the same system reported by Lee et al. (*p*-xylene in FCC catalyst) indicates that the invariance of the adsorption/desorption dynamics on carrier gas flow rate does not necessarily imply that the concentration gradient down the packed bed is negligible. For a certain sample size ($\leq\sim$64 mg), the transient adsorption/desorption profiles at 373 K and *p*-xylene partial pressure of 0.006 bar overlap with each other when the carrier gas flow rate is $\geq$ 400 sccm. However, at the carrier gas flow rate of 400 sccm, the adsorption/desorption dynamics are strongly influenced by sample size, as shown in Figure 8. The adsorption/desorption rates for smaller sample sizes are higher under otherwise identical conditions, clearly demonstrating the significance of bed-length effect on the observed dynamics during TEOM experiments.

The transient adsorption/desorption profiles of isobutane, *n*-butane, and propane in β- and USY-zeolite crystals were measured under adsorbate partial pressures of 0–1.1 bar at temperatures of 303–398 K. The effects of carrier gas flow rate and sample size on adsorption/desorption profiles were investigated (Figures 9 and 10). At 323 K, isobutane partial pressure of 0.015 bar and a sample size of 7.4 mg, the adsorption/desorption profiles become invariant with flow beyond 333 sccm (Figure 9). However, further experiments with decreased sample size clearly demonstrate that sample

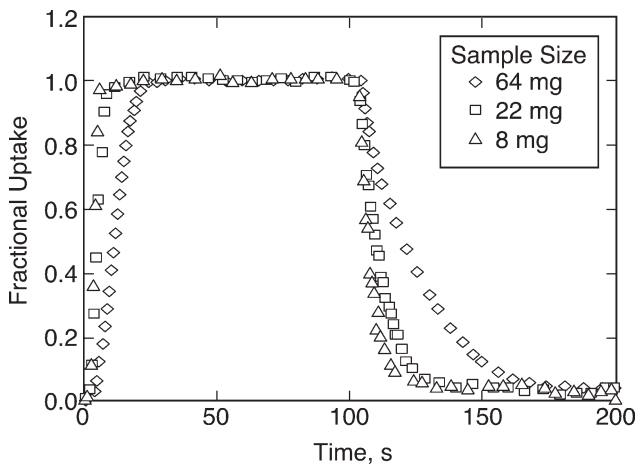

Figure 8. Effect of sample size on sorption profiles for *p*-xylene in FCC catalyst (T = 373 K, carrier gas is helium flowing at 400 sccm, P_{total} = 1.01 bar, $P_{p\text{-xylene}}$ = 0.006 bar).

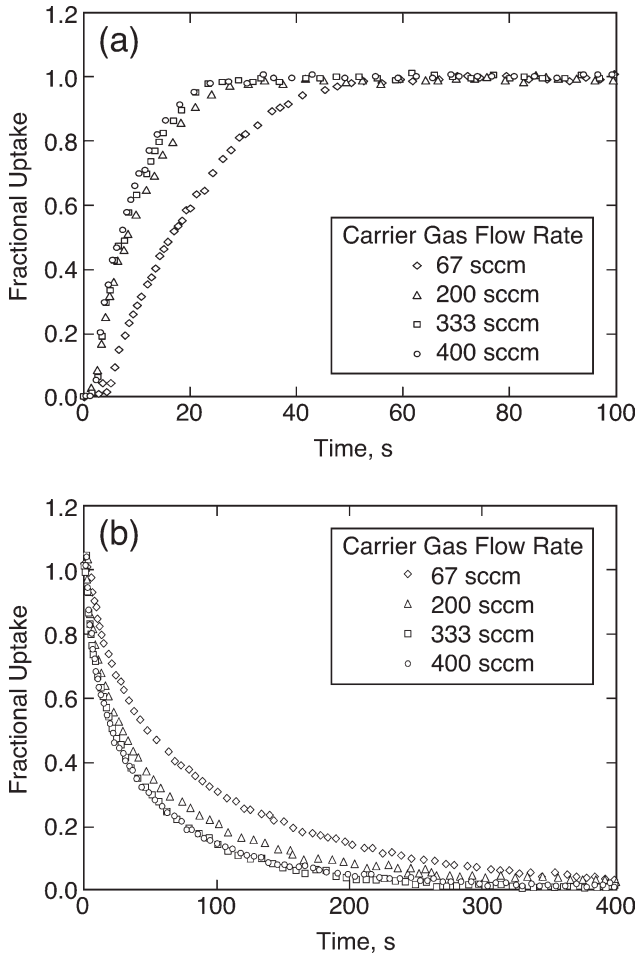

Figure 9. Effect of carrier gas (He) flow rate on sorption profiles for isobutane in β-zeolite (T = 323 K, P_{iC4} = 0.015 bar, P_{total} = 1.01 bar, sample size = 7.4 mg) (a) adsorption profiles, and (b) desorption profiles.

size effects are significant even at the highest carrier gas flow rate of 400 sccm (Figure 10). These results reinforce the fact that the absence of bed-length effects in TEOM studies must be confirmed by varying both the flow rate, as well as the sample size.

The mathematical model for intracrystalline diffusion control was used to fit the isobutane sorption profiles in β-zeolite with a sample size of 1.6 mg at a helium flow rate of 400 sccm at 323 K, conditions under which the bed-length effect and external film resistance are minimized. As shown in Figure 11, the model represents the experimental profile reasonably well, with the corrected intracrystalline diffusivity (D_0) of 8×10^{-12} cm^2/s. In sharp contrast, the intracrystalline diffusivity of *n*-butane in large-pore (12-ring) zeolites measured by other techniques using large crystals[9] are 3–4 orders of magnitude higher than the value obtained in this study, implying that an additional mass transfer resistance, rather than intracrystalline diffusion alone, is likely dominant in our measurements. Notice that the samples employed in this work are aggregated crystals, and the agglomeration of crystals could possibly impose a significant extracrystalline

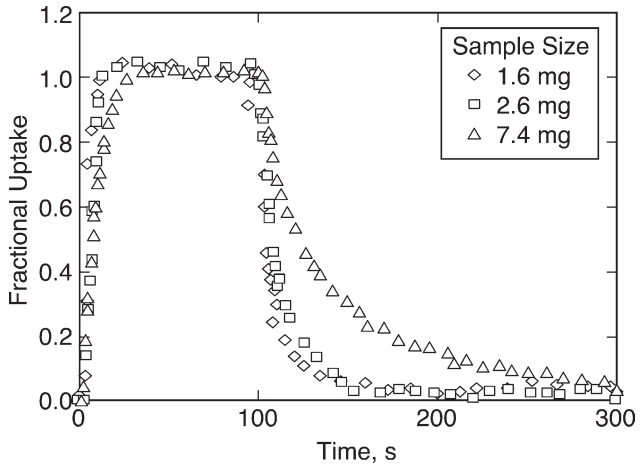

Figure 10. Effect of sample size on sorption profiles for isobutane in β-zeolite (T = 323 K, carrier gas is helium flowing at 400 sccm, P_{iC4} = 0.015 bar, P_{total} = 1.01 bar).

mass transfer limitation. Such a possibility is investigated in the following section.

Effect of Crystal Agglomeration. To study the effect of crystal agglomeration on the sorption dynamics, pelletized zeolite samples were employed. The pellets were formed by pressing the powder-form zeolites under ~7 MPa pressure into 3.5-mm-thick, 3.5-mm diameter cylinders. The transient sorption profiles of isobutane, *n*-butane, and propane were each investigated in pelletized β- and USY-zeolite samples under adsorbate partial pressures in the 0–1.1 bar range, and at temperatures in the 303–398 K range. The adsorption/desorption profiles were measured over small concentration steps, such that the rates of desorption and adsorption are identical.

It is found that the sorption curves merge with each other when plotted vs. t/R_p^2 (Figure 12). This implies that mesopore/macropore diffusion resistance, introduced by the

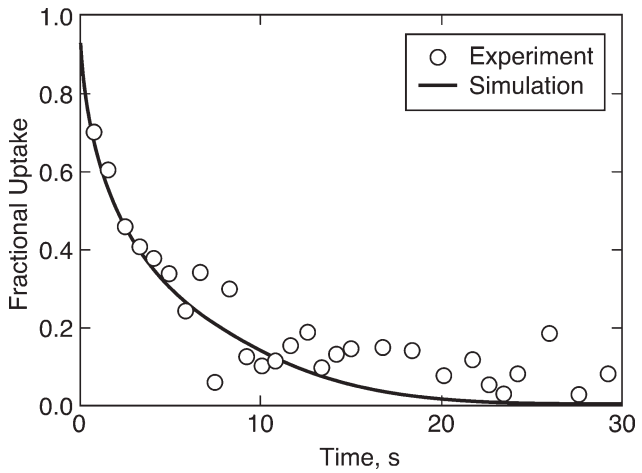

Figure 11. Experimental and simulated desorption profiles for isobutane in β-zeolite (T = 323 K, carrier gas is helium flowing at 400 sccm, P_{total} = 1.01 bar, P_{iC4} = 0.015–0 bar).

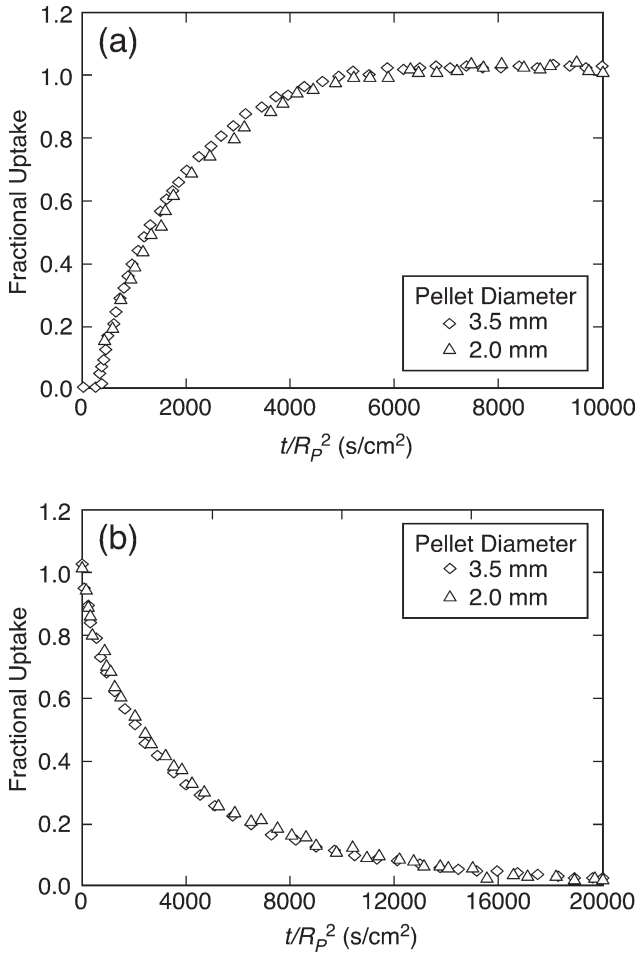

Figure 12. Effect of pellet size on sorption profiles for isobutane in β-zeolite (T = 323 K, carrier gas is helium flowing at 400 sccm, P_{total} = 1.01 bar, P_{iC4} = 0.005 bar), (a) adsorption profiles, and (b) desorption profiles.

pelletization step, is dominant.[9,28] Similar investigations have been reported in the literature to study the effect of crystal agglomeration on observed kinetics. For example, Ruthven and Xu[32] confirmed that the mesopore/macropore diffusion is the rate-limiting step for oxygen and nitrogen adsorption/desorption in commercial 5A pellets using different particle size fractions by the ZLC method. Using a conventional electrobalance, Youngquist et al.[33] investigated butylene adsorption/desorption in calcium microtraps of different sizes and found that the extracrystalline transport is rate limiting.

The adsorption/desorption profiles were regressed with a solution of the mesopore/macropore-diffusion-controlled model to obtain effective mesopore/macropore diffusivities. The model fits the sorption curves reasonably well, as shown in Figure 13. The concentration dependence of effective diffusivity under the conditions of mesopore/macropore diffusion control is shown in Figure 14. At a given temperature, the effective mesopore/macropore diffusivity increases with adsorbate loading, mainly due to the decreasing slope of the equilibrium adsorption isotherm (dq^*/dc).[9] The pore diffusivities (D_p) can be calculated from the effective mesopore/macropore diffusivities using the values of ε_p (obtained from porosimetry), and dq^*/dc (derived from the equilibrium adsorption isotherms), and the dependence of pore diffusivities on adsorbate concentration or pressure can be further studied.[9]

Limitations of the TEOM Technique for Diffusivity Measurement. In principle, there is an upper limit of the diffusional time constant (D/R^2) that the TEOM technique can measure. Above the limit, the diffusion is too rapid, and the contribution from the inevitable mixing and time delay due to dead volume in the system becomes dominant, rendering it impossible to obtain reliable diffusion dynamics data.

When there is negligible adsorption (as when using nonporous quartz particles), the response curve is fairly close to an ideal step due to the small dead volume in the system. The new equilibrium state is obtained within 2–4 s after a step change reaches the packed bed in a TEOM.[22] Therefore, the sorption time should be at least 20 s so that the dead volume effects can be considered insignificant. Such a time frame corresponds to an approximate value of $D/R^2 = 0.02$ s^{-1} for a spherical particle.[28] Consequently, a reasonable criterion for reliable measurement of the diffusional time constant by the TEOM technique is: $D/R^2 < 0.02$ s^{-1}. An almost identical criterion was used by Kärger and Ruthven[9] for the ZLC technique, and was demonstrated to be useful for properly choosing the operating conditions in the diffusivity measurements.

At 298–373 K, the intracrystalline diffusivity of *n*-butane in large-pore (12-ring) NaX zeolites with large crystals is determined to be of order 10^{-7} cm^2/s by classic macroscopic methods (e.g., the ZLC and gravimetric methods).[9] Assuming that *n*-butane has similar diffusivities in the commercial β-zeolite and USY-zeolite crystals (<1 μm), the diffusion time scale will be of order 2.5×10^{-2} s, which is not measurable by the TEOM technique. The intracrystalline diffusivity can only be reliably extracted from the transient

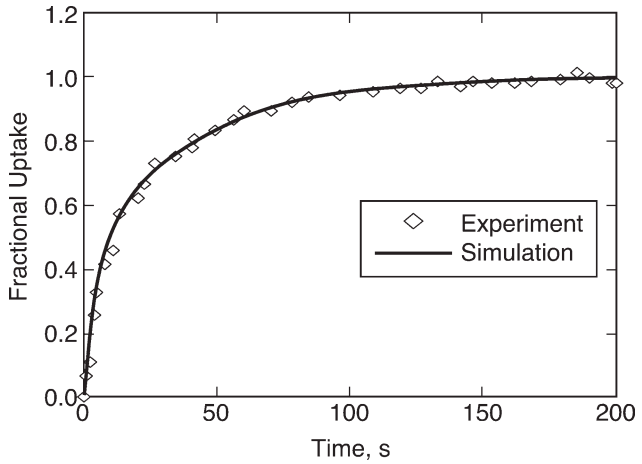

Figure 13. Experimental and simulated uptake curves for isobutane in β-zeolite pellets (T = 348 K, carrier gas is helium flowing at 400 sccm, P_{total} = 1.01 bar, P_{iC4} = 0.005–0.0075 bar).

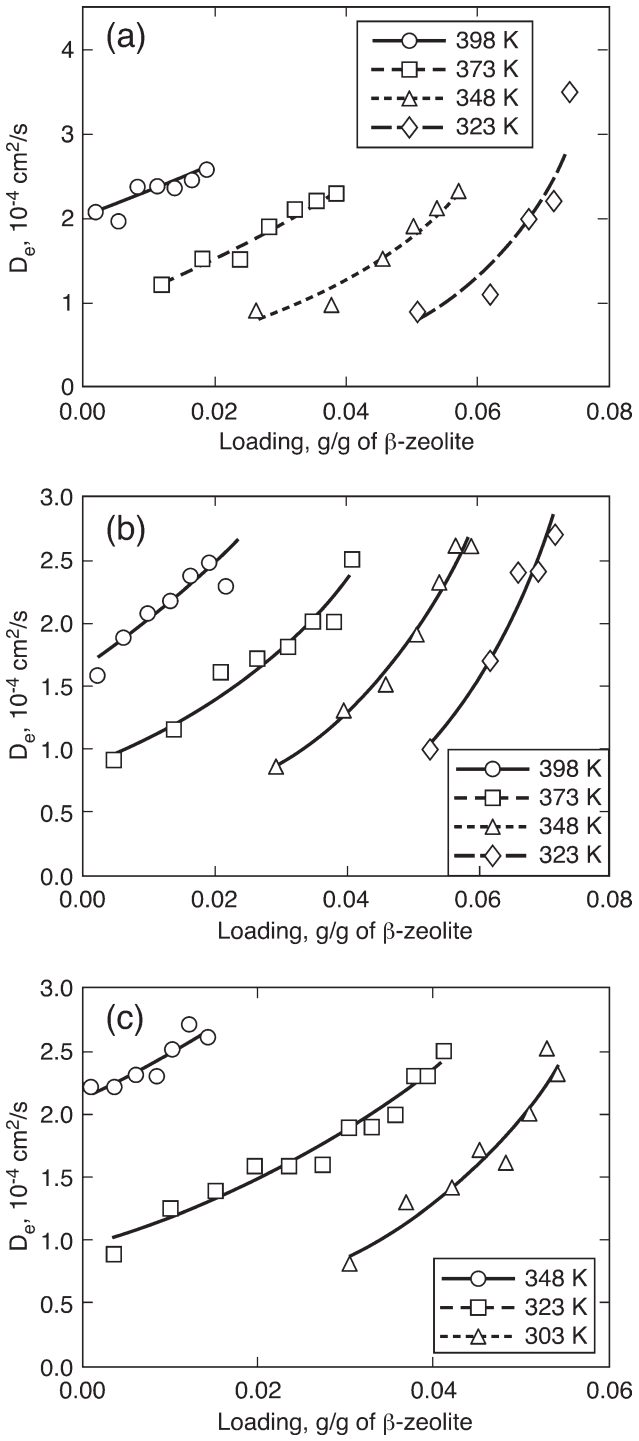

Figure 14. Concentration dependence of effective mesopore/macropore diffusivity (carrier gas is helium flowing at 400 sccm, P_{total} = 1.01 bar): (a) isobutane in β-zeolite pellets, (b) *n*-butane in β-zeolite pellets, and (c) propane in β-zeolite pellets.

measurements by the TEOM technique when the crystal size of these zeolites is larger than 44 μm.

In our studies of isobutane, *n*-butane, and propane adsorption/desorption in pelletized zeolite samples, the measured effective mesopore/macropore diffusivity is on the order of 10^{-4} cm^2/s, and the diffusion time scale for the 2 mm pellet is on the order of 100 s. When the pellet diameter is less than 1.4 mm, the diffusivity measurements using the TEOM become unreliable.

Conclusions

The TEOM is demonstrated as a useful tool to measure the adsorption equilibria and adsorption/desorption dynamics of hydrocarbons in porous catalysts, and a deeper understanding of adsorption/desorption characteristics of alkylation reactants on zeolites is successfully gained.

At typical temperatures (303–398 K) reported in the literature for solid acid alkylation catalysis, the equilibrium adsorption isotherms of isobutane, *n*-butane, and propane in USY-zeolite are fitted well by Langmuir model. However, for the same molecules, the dual-site Langmuir model is a better descriptor of the adsorption isotherms in β-zeolite at relatively low temperatures, indicating the existence of perhaps two types of adsorption sites.

Investigations into adsorption/desorption dynamics in large-pore (12-ring) zeolite crystals (<1 μm) reveal that the corrected intracrystalline diffusivity of isobutane in β-zeolite, estimated from TEOM experiments and complementary single particle model describing simultaneous diffusion and adsorption, is 3-4 orders of magnitude lower than the literature values of similar systems. This implies that an additional mass transfer resistance, other than just the intracrystalline diffusion resistance, is also influencing the measurements. Designed investigations with pelletized zeolite samples, ranging from 2.0 to 3.5 mm, conclusively show that transport resistances in the extra-crystalline meso- and macropores control the adsorption and desorption dynamics. The experimental adsorption/desorption profiles from the pelletized zeolites were regressed with available mathematical models to obtain effective mesopore/macropore diffusivities for reactant molecules such as isobutane, *n*-butane and propane. At a given temperature, the effective mesopore/macropore diffusivity (resulting from the nearly perfect fits of the experimental and the modeled profiles) increases with adsorbate loading, mainly due to the decreasing slope of the equilibrium adsorption isotherm. Similar to the zero length column (ZLC) method, the TEOM technique requires the diffusion time scales in the pores to be slow enough for reliable measurement with minimal or insignificant signal dampening from the system dead-volume and dispersion effects. An order of magnitude analysis indicates that a reasonable criterion for reliable measurements of the diffusion time constants by the TEOM technique is $D/R^2 < 0.02$ s^{-1}.

Acknowledgments

This research was supported with funds provided by the Center for Environmentally Beneficial Catalysis under the National Science Foundation Engineering Research Centers Grant (EEC-0310689). We also thank Richard B. Maynard and Dana M. Jones of DuPont for performing the catalyst surface area and pore volume measurements, and Dr. Joe Allison and Dr. Jane Yao of ConocoPhillips for their support on the ammonia TPD characterization of the samples.

Literature Cited

1. Corma A, Martinez A. Chemistry, catalysts, and processes for isoparaffin-olefin alkylation - Actual situation and future trends. *Catal Rev*. 1993;35:483–570.
2. deJong KP, Mesters CMAM, Peferoen DGR, vanBrugge PTM, de Groot C. Paraffin alkylation using zeolite catalysts in a slurry reactor: Chemical engineering principles to extend catalyst lifetime. *Chem Eng Sci*. 1996;51:2053–2060.
3. Weitkamp J, Traa Y. Isobutane/butene alkylation on solid catalysts. Where do we stand? *Catal Today*. 1999;49:193–199.
4. Platon A, Thomson WJ. Solid acid characteristics and isobutane/butene alkylation. *Appl Catal A: Gen*. 2005;282:93–100.
5. Yoo K, Burckle EC, Smirniotis PG. Comparison of protonated zeolites with various dimensionalities for the liquid phase alkylation of *i*-butane with 2-butene. *Catal Lett*. 2001;74:85–90.
6. Sarsani VSR, Subramaniam B. Isobutane/butene alkylation on microporous and mesoporous solid acid catalysts: Probing the pore transport effects with liquid and near critical reaction media. *Green Chem*. 2009;11:102–108.
7. Nivarthy GS, He YJ, Seshan K, Lercher JA. Elementary mechanistic steps and the influence of process variables in isobutane alkylation over H-BEA. *J Catal*. 1998;176:192–203.
8. Gong K, Shi T, Ramachandran PA, Hutchenson KW, Subramaniam B. Adsorption/desorption studies of 224-trimethylpentane in β-zeolite and mesoporous materials using a tapered element oscillating microbalance (TEOM). *Ind Eng Chem Res*. published online July 28, 2009; DOI: 10.1021/ie900334g
9. Kärger J, Ruthven DM. *Diffusion in zeolites and other microporous solids*. New York: Wiley; 1992.
10. Wang JCF, Patashnick H, Rupprecht G. A new real-time isokinetic dust mass monitoring system. *J Air Pollution Control Assn*. 1980; 30:1018–1021.
11. Patashnick H, Rupprecht G. New real-time monitoring instrument for suspended particulate mass concentration - TEOM. *Abstr Pap Am Chem S*. 1980;179:51–51.
12. Chen D, Gronvold A, Rebo HP, Moljord K, Holmen A. Catalyst deactivation studied by conventional and oscillating microbalance reactors. *Appl Catal A: Gen*. 1996;137:L1–L8.
13. Liu K, Fung SC, Ho TC, Rumschitzki DS. Kinetics of catalyst coking in heptane reforming over Pt-Re/Al_2O_3. *Ind Eng Chem Res*. 1997;36:3264–3274.
14. Chen D, Rebo HP, Moljord K, Holmen A. Methanol conversion to light olefins over SAPO-34. Sorption, diffusion, and catalytic reactions. *Ind Eng Chem Res*. 1999;38:4241–4249.
15. Chen D, Rebo HP, Moljord K, Holmen A. Influence of coke deposition on selectivity in zeolite catalysis. *Ind Eng Chem Res*. 1997; 36:3473–3479.
16. Hershkowitz F, Madiara PD. Simultaneous measurement of adsorption, reaction, and coke using a pulsed microbalance reactor. *Ind Eng Chem Res*. 1993;32:2969–2974.
17. van Donk S, Broersma A, Gijzeman OLJ, van Bokhoven JA, Bitter JH, de Jong KP. Combined diffusion, adsorption, and reaction studies of *n*-hexane hydroisomerization over Pt/H-mordenite in an oscillating microbalance. *J Catal*. 2001;204:272–280.
18. Chen D, Rebo HP, Moljord K, Holmen A. Effect of coke deposition on transport and adsorption in zeolites studied by a new microbalance reactor. *Chem Eng Sci*. 1996;51:2687–2692.
19. Rebo HP, Chen D, Brownrigg MSA, Moljord K, Holmen A. Adsorption and diffusion in HZSM-5 zeolite studied by an oscillating microbalance. *Collect Czech Chem Commun*. 1997;62:1832–1842.
20. Chen D, Rebo HP, Holmen A. Diffusion and deactivation during methanol conversion over SAPO-34: A percolation approach. *Chem Eng Sci*. 1999;54:3465–3473.
21. Alpay E, Chadwick D, Kershenbaum LS, Barrie PJ, Sivadinarayana C, Gladden LF. TEOM analysis of the equilibria and kinetics of *n*-hexane and *n*-heptane adsorption on FCC catalyst/silicalite. *Chem Eng Sci*. 2003;58:2777–2784.
22. Lee CK, Ashtekar S, Gladden LF, Barrie PJ. Adsorption and desorption kinetics of hydrocarbons in FCC catalysts studied using a tapered element oscillating microbalance (TEOM). Part 1: Experimental measurements. *Chem Eng Sci*. 2004;59: 1131–1138.
23. Barrie PJ, Lee CK, Gladden LF. Adsorption and desorption kinetics of hydrocarbons in FCC catalysts studied using a tapered element oscillating microbalance (TEOM). Part 2: Numerical simulations. *Chem Eng Sci*. 2004;59:1139–1151.
24. Zhu W, Kapteijn F, Moulijn JA. Diffusion of linear and branched C_6 alkanes in silicalite-1 studied by the tapered element oscillating microbalance. *Micropor Mesopor Mater*. 2001;47:157–171.
25. Zhu W. *Adsorption and diffusion in microporous materials: An experimental study with the TEOM*. Delft University of Technology, Delf; 2001. Ph.D Dissertation.
26. Zhu W, van de Graaf JM, van den Broeke LJP, Kapteijn F, Moulijn JA. TEOM: A unique technique for measuring adsorption properties. Light alkanes in silicalite-1. *Ind Eng Chem Res*. 1998;37:1934–1942.
27. Barcia PS, Silva JAC, Rodrigues AE. Separation by fixed-bed adsorption of hexane isomers in zeolite BETA pellets. *Ind Eng Chem Res*. 2006;45:4316–4328.
28. Duong DD. *Adsorption analysis: Equilibria and kinetics*. London, River Edge, NJ: Imperial College Press; 1998.
29. Hyun HS, Danner PR. Equilibrium adsorption of ethane, ethylene, isobutane, carbon dioxide, and their binary mixtures on 13X molecular sieves. *J Chem Eng Data*. 1982;27:196–200.
30. Costa E, Galleja G, Jimenez A, Pau J. Adsorption equilibrium of ethylene, propane, propylene, carbon dioxide, and their mixtures on 13X zeolite. *J Chem Eng Data*. 1991;36:218–224.
31. Suzuki M. *Adsorption Engineering*. Tokyo: Kodansha; Elsevier; 1990.
32. Ruthven DM, Xu Z. Diffusion of oxygen and nitrogen in 5A zeolite crystals and commercial 5A pellets. *Chem Eng Sci*. 1993;48:3307–3312.
33. Youngquist RG, Allen JL, Eisenberg J. Adsorption of hydrocarbons by synthetic zeolites. *Ind Eng Chem Prod Res Dev*. 1971;10:308–314.

Manuscript received Mar. 30, 2009, and revision received July 22, 2009.